crystals

MDPI

Article

Influence of Deposition Time on Properties of Se-Doped CdTe Thin Films for Solar Cells

Ibrahim M. Beker [1,*], Francis B. Dejene [1], Lehlohonolo F. Koao [2], Jacobus J. Terblans [3] and Habtamu F. Etefa [1]

[1] Department of Chemical and Physical Sciences, Faculty of Natural Sciences, Walter Sisulu University, Mthatha Campus, Nelson Mandela Drive Private Bag X1, Mthatha 5117, South Africa; fdejene@wsu.ac.za (F.B.D.); hetefa@wsu.ac.za (H.F.E.)
[2] Department of Physics, University of the Free State (QwaQwa Campus), Private Bag X13, Phuthaditjhaba 9866, South Africa; koaolf@ufs.ac.za
[3] Department of Physics, University of the Free State, Bloemfontein P.O. Box 339, South Africa; terblansjj@ufs.ac.za
* Correspondence: 231177348@mywsu.ac.za

Abstract

Se-doped CdTe thin films were grown employing a simple two-electrode electrochemical deposition method using glass/tin-doped indium oxide (glass/ITO). Cadmium acetate dihydrate [Cd $(CH_3CO_2)_2$. $2H_2O$], selenium dioxide (SeO_2), and tellurium dioxide (TeO_2) were used as precursors. Instruments including X-ray diffraction for structural investigation, UV-Vis spectrophotometry for optical properties, and scanning probe microscopy for morphological properties were employed to investigate the physico-chemical characteristics of the resulting Se-doped CdTe thin-film. The films are polycrystalline with a cubic phase, according to X-ray diffraction (XRD) data. More ions are deposited on the substrate, which makes the material more crystalline and intensifies the characteristic peaks that are seen. It is observed from the acquired optical characterization that the film's bandgap is greatly influenced by the deposition time. The bandgap dropped from 1.92 to 1.62 as the deposition period increased from 25 to 45 min, making the film more transparent and absorbing less light at shorter deposition durations. Images from scanning electron microscopy (SEM) show that the surface morphology is homogenous with closely packed grains and that the grain forms become less noticeable as the deposition time increases. This work is novel in that it investigates the influence of the deposition time on the structural, optical, and morphological properties of Se-doped CdTe thin films deposited using a cost-effective, simplified two-electrode electrochemical method—a fabrication route that remains largely unexplored for this material system.

Keywords: electrodeposition; deposition time; CdTe:Se; surface morphology; solar cell

check for updates

Academic Editor: Vladislav V. Kharton

Received: 31 May 2025
Revised: 18 June 2025
Accepted: 20 June 2025
Published: 22 June 2025

Citation: Beker, I.M.; Dejene, F.B.; Koao, L.F.; Terblans, J.J.; Etefa, H.F. Influence of Deposition Time on Properties of Se-Doped CdTe Thin Films for Solar Cells. *Crystals* **2025**, *15*, 589. https://doi.org/10.3390/cryst15070589

Copyright: © 2025 by the authors. Licensee MDPI, Basel, Switzerland. This article is an open access article distributed under the terms and conditions of the Creative Commons Attribution (CC BY) license (https://creativecommons.org/licenses/by/4.0/).

1. Introduction

Cadmium telluride thin-film solar cells' low cost, high-rate deposition, and long-term stability make them attractive options for producing power on a big scale on land. There have undoubtedly been two distinct paths taken in the development of CdTe thin-film solar cells in recent years [1]. On the one hand, scientists are working to change the high-energy and material-intensive manufacturing procedures of the past by creating devices with thinner absorbers that are deposited using low-temperature fabrication techniques. The low-cost manufacturing process is important for applications using multi-layer solar cells with higher efficiency [2,3]. Conversely, conventional CdTe solar cells have demonstrated

a notable increase in efficiency, enhancing their potential for commercial exploitation. Theoretical calculations estimate a maximum efficiency of around 30%, while experimental efforts have achieved record efficiencies of up to 22.1%. This positions CdTe technology as a compelling alternative when compared to the widely adopted silicon-based solar cells [4]. In recent years, several methods have been put forth and implemented to maximize the solar cell's parameters, including fill factor (FF), open circuit voltage (V_{oc}), and short circuit current density (J_{sc}), to boost efficiency [5,6]. Recently, there has been a greater focus on improving the J_{sc} values. The addition of Se to the CdTe absorber layer structure produced the best results, even though other strategies, such as more transparent window layers, were assessed to raise the short circuit current density [3,5].

The rise of ground-based solar cells can be attributed to the availability and great thermal and chemical stability of cadmium telluride (CdTe). This, however, faces the issue of forming reliable ohmic contacts with CdTe and increasing power conversion efficiency for solar devices. The photovoltaic CdTe cells also retain a unique advantage in that their band gap coincides well with the peak intensity of solar irradiation, making them favorable for the harvest and conversion of solar energy [7,8].

A thin CdSexTe1-x interlayer is said to be beneficial when placed close to the interface between the CdTe absorber and the CdS junction partner. The typical CdTe solar cell structure has a near-junction, a defective region causing photocurrent loss in the cell through recombination. The typical CdS junction partner and CdTe film have different lattices, which is one cause. At this interface, the presence of a $CdSe_xTe_{1-x}$ layer decreases the carrier recombination and lattice mismatch at the grain boundaries and close to the interface [9,10]. Another factor to consider is that lower energy photons can be absorbed by this inter-layer and contribute to the photocurrent because of the reduced band gap of $CdSe_xTe_{1-x}$. Additionally, $CdSe_xTe_{1-x}$ improves the absorber's electrical characteristics, including the diffusion length and charge carrier lifetime, to boost cell performance. Adding Se to the device structure frequently results in the creation of a Junction Partner/$CdSe_xTe_{1-x}$/CdTe/Back-Contact array [3,11,12]. This study emphasizes how crucial a well-understood and compositionally well-regulated CdSeTe layer—specifically in terms of stoichiometric control and uniformity—is to the ongoing improvement of the CdTe photovoltaic device performance.

Numerous deposition methods, including molecular beam epitaxy [13], electron beam evaporation [14], hot wall deposition [15], thermal evaporation [16], close-spaced sublimation (CSS) [17] and metal-organic chemical vapor deposition (MOCVD) [18], and electrodeposition [19], have been used in the synthesis of CdTe:Se thin films.

While every deposition method has pros and cons of its own, electrodeposition offers special benefits over other solution-based methods. One of the main problems with these solution-based methods, especially CBD, is that the solution is used up after only one round of deposition and more resources are required to dispose of the waste chemical. In contrast, electrodeposition eliminates the requirement for periodic waste chemical disposal by allowing the electrolyte to be utilized for extended periods of time—up to several months—by only filtering the electrolytic solution when precipitation occurs. As the ion concentration decreases throughout this process, the current density will also drop, and estimated quantities of ion-containing compounds from the stock solutions are added. Additionally, the electrolytic bath becomes purified as the electroplating process advances due to the slow elimination of contaminants [20].

Conversely, alternative wet chemical-based methods, such as CBD, employ complexing agents to form complexes of the pertinent ions for convenient release; but, once the reaction starts, it is hard to regulate it and, therefore, the thickness of the developing sample. To build a sample with the desired thickness and homogeneity, however, electrodeposi-

tion makes it simple to monitor the deposition rate by just changing the stirring rate and keeping an eye on the current density. Several studies on the independent development of CdTe and CdSe utilizing the electrodeposition technique have been conducted [21,22]. Nevertheless, there is a dearth of research on the electrodeposition method for CdTe:Se thin film deposition. Consequently, the electrodeposition approach was used in this study to generate CdTe:Se thin films for potential use in solar cells. In addition, in the study, the process was simplified by employing a basic two-electrode configuration instead of the conventional three-electrode system. In the event of a leaky or damaged reference electrode, this aids in the removal of the reference electrode, which often includes KCl, which is a p-type dopant in II-VI semiconductors and can contaminate the deposition bath.

The quality of the deposited films is strongly influenced by the optimization of various deposition parameters, such as the deposition time, electrolyte bath temperature, ion concentration, pH level, stirring conditions, applied voltage, and the type of electrodes used [23]. Not enough research has been conducted on how the deposition time affects the characteristics of CdTe:Se thin films among these deposition parameters.

In the literature, it is known that the deposition time needed to grow CdTe is quite different from that needed to grow CdSe [24,25]. Therefore, the deposition time used to produce the CdTe:Se has a major impact on the thin film's stoichiometry and quality. This article aims to address the aforementioned research gap by carefully selecting all other deposition parameters and examining the impact of the deposition time on the structural, optical, compositional, and morphological characteristics of electroplated CdTe:Se thin film.

2. Materials and Methods

Electrolytic Solution Preparation

The electrolyte solution used for the growth of CdTe:Se thin films comprised the following precursors: 1.0 M cadmium acetate dihydrate [$Cd(CH_3CO_2)_2 \cdot 2H_2O$] with 98% purity as the cadmium source, 0.01 M selenium dioxide (SeO_2) with 98% purity as the selenium source, and 1 mL of tellurium dioxide (TeO_2) with 99% purity as the tellurium source. Thin films were deposited using a two-electrode electrodeposition (ED) technique on glass substrates coated with indium tin oxide (ITO), exhibiting a sheet resistance of 15–25 Ω/sq. All the chemicals used in the experiment were from Sigma-Aldrich (Merck KGaA), Darmstadt, Germany. The glass/ITO was ultrasonically cleaned for 30 min using a solution of laboratory soap in deionized water, and then cleaned sequentially with ethanol, acetone, and methanol before electrodeposition. After being washed with deionized water in between washings, the substrate was let to air dry. The electrolyte solution's pH was adjusted to 2.5 using room-temperature diluted acetic acid. During the deposition process, a magnetic stirrer was used to gently mix the electrolyte solution while maintaining the deposition temperature of the electrolyte solution bath at 75 °C. The Gill AC potentiostatic, manufactu red by ACM Instruments in the United Kingdom, was the computerized power source for the two-electrode system.

The ITO/glass substrate was secured over the operating high-purity electrode (cathode) using an insulating polytetrafluoroethylene (PTFE) thread seal tape. Prior to CdTe:Se thin film deposition, 600 mL of a beaker held cadmium acetate solution that was electropurified for 48 h. Deposition was performed at a voltage below that required for the reduction of elemental cadmium, which was investigated using a cyclic voltammetry analysis. The Te-containing solution was separately prepared with 2 g dissolution of TeO_2 in 30 mL of diluted HCl and then stirring for 120 min. Though tellurium is insoluble in water, it is soluble in acidic environments. For preparing the homogeneous precursor solution, 1 mL of Te-containing solution was added to the Cd- and Se-containing solution and repeatedly stirred for a further 5 hours.

A cathode voltage of 1890 mV was then used to deposit the CdTe:Se thin film. The conductive glass substrate that was washed first was immersed in the electrolyte solution for 25, 35, 45, and 55 min. A slight stirring of the solution was required for the deposition process. Following the sample's extraction from the solution, it was rinsed with deionized water and allowed to air-dry. Later, the CdTe:Se thin films that were deposited using a simple two-electrode electrodeposition setup, as illustrated in Figure 1, were assessed in terms of their structure, optical property, surface morphology, and elemental content.

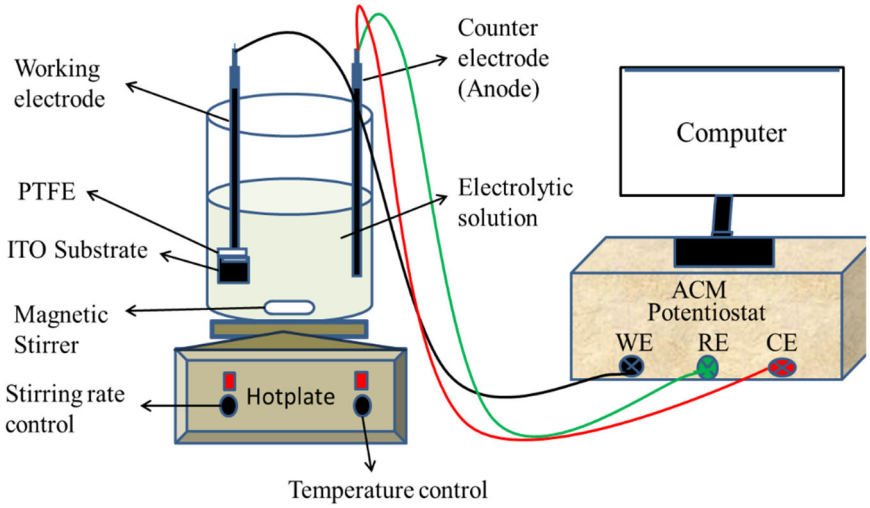


Figure 1. CdTe:Se thin film grown using a simple two-electrode electrodeposition setup.

X-ray diffraction (XRD) analysis was conducted to examine the structural properties and phase composition of the thin film samples using a Bruker D8 Advance Powder Diffractometer fitted with an SSD160-1D mode detector (Bruker AXS GmbH, Karlsruhe, Germany). Optical absorbance spectra were obtained using a Lambda 950 UV-Vis spectrophotometer (PerkinElmer, Waltham, MA, USA). An Oxford Aztec 350 X-Max 80 energy dispersive X-ray spectrometer (EDS) (Oxford Instruments, Abingdon, Oxfordshire, UK) was utilized in conjunction with a Jeol JSM7800F field emission scanning electron microscope (FESEM) (JEOL Ltd., Tokyo, Japan) to examine the morphology and elemental makeup of thin films. The surface roughness characteristics of the thin films were examined with a scanning probe microscope (SPM) (9600 Shimadzu Corporation, Kyoto, Japan).

3. Results and Discussion

3.1. Structural Properties

To assess the structural and phase purity of electrodeposited CdTe:Se thin films, XRD was performed using a Bruker D-8 Advanced X-ray Diffractometer. Throughout the testing, the voltage and current remained at their set levels of 40 kV and 40 mA, respectively. The 2θ angle range was 20°–70°. Figure 2 shows the XRD patterns of the CdTe:Se thin films grown at different deposition times. The results indicate that the peak position and intensity of the measured data and the JCPDS reference file number 75-2086 coincide to a good extent.

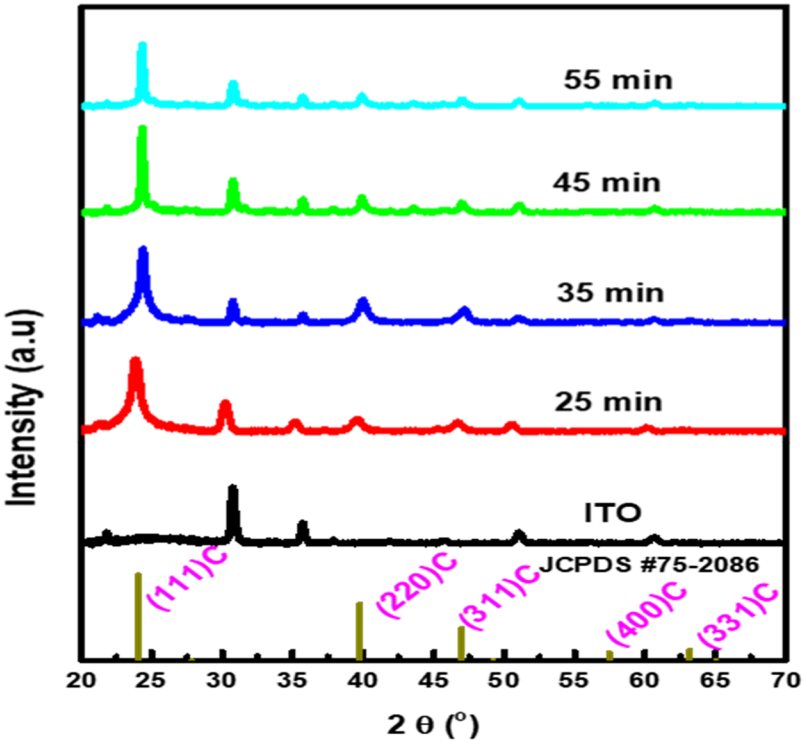


Figure 2. XRD patterns of CdTe:Se films grown at different deposition times.

With 2θ values of 24.03, 39.77, and 46.97, respectively, the films display peaks with a preferred orientation (111), (220), and (311). XRD peaks observed at 2θ values of 21.77°, 30.73°, 35.67°, 51.04°, and 60.71° correspond to the glass substrate (ITO). According to the data, the formed CdTe:Se thin film exhibits cubic phase peaks at all deposition times. The intensity of the (111) peak rises with higher deposition times; the maximum peak was seen at 45 min before it started to decrease. Other research by Çiriş et al. [26] focuses on the effect of deposition parameters on the shutter control index for the shape and structure features of the CdSeTe films. In the case where the substrate temperature was controlled, their findings suggest that an increased temperature resulted in higher grain sizes and more uniform surfaces, which correlates with our findings on the deposition time in our studies on CdTe:Se thin films. The following formulae are utilized to calculate crystallite sizes (D) from the Scherrer equation, interplanar spacings (d_{hkl}) using Bragg's diffraction equation, and lattice constants (a) using the formula for a cubic system [23]:

$$D = \frac{0.94\lambda}{\beta cos\theta} \quad (1)$$

$$d_{hkl} = \frac{n\lambda}{2sin\theta} \quad (2)$$

$$\left(\frac{1}{d_{hkl}}\right)^2 = \frac{h^2 + k^2 + l^2}{a^2} \quad (3)$$

The dislocation density (δ) and micro strain (ε) of the thin films were estimated using the following relationships [27].

$$\delta = \frac{1}{D^2} \quad (4)$$

$$\varepsilon = \frac{\beta}{4tan\theta} \quad (5)$$

where n is a positive integer, θ represents the diffraction angle, β denotes the full width at half maximum (FWHM) of the diffraction peak, λ is the wavelength of the X-ray source, and *(hkl)* corresponds to the Miller indices as identified from the JCPDS reference data.

The average crystallite sizes (D) corresponding to the peak intensities (111) of the deposition times recorded at 25, 35, 45, and 55 min were 12.65 nm, 15.77 nm, 25.77 nm, and 17.21 nm, respectively, as shown in Table 1.

Table 1. From the XRD measurement data, the diffraction angle, (*hkl*) values, **d**-spacing, β, crystallite sizes (D), dislocation density, and micro strain were determined.

Time (min)	2 θ (°)	(*hkl*)	β (°)	D (nm)	$D_{av.}$	$\delta \times 10^{11}$ cm^{-2}	δ_{av}	ε	$\varepsilon_{av.}$
25	23.89	(111)	0.569	14.92	12.65	4.5		0.67	
	39.63	(220)	0.746	11.82		7.2	6.5	0.52	0.55
	46.78	(311)	0.807	11.20		8.0		0.47	
35	23.98	(111)	0.515	16.46	15.77	3.7		0.61	
	39.98	(220)	0.581	15.20		4.3	4.0	0.40	0.45
	47.01	(311)	0.578	15.65		4.1		0.33	
45	24.03	(111)	0.251	33.80	25.77	0.9		0.29	
	39.77	(220)	0.379	23.28		1.8	1.7	0.26	0.27
	46.97	(311)	0.447	20.23		2.4		0.26	
55	23.95	(111)	0.425	19.95	17.21	2.5		0.50	
	39.71	(220)	0.564	15.64		4.1	3.5	0.39	0.41
	46.73	(311)	0.564	16.04		3.9		0.33	

The lattice parameter (a) of the deposited CdTe:Se films were found to range between 6.41 Å and 6.45 Å, which is in good agreement with the standard value of 6.41 Å reported in the JCPDS data card No. 75-2086.

As the deposition time increases, the dislocation density drops, reaching its lowest at 45 min, as seen in Figure 3a. The dislocation density is maximum at a short deposition time of 25 min. At 55 min, the dislocation density slightly increased.

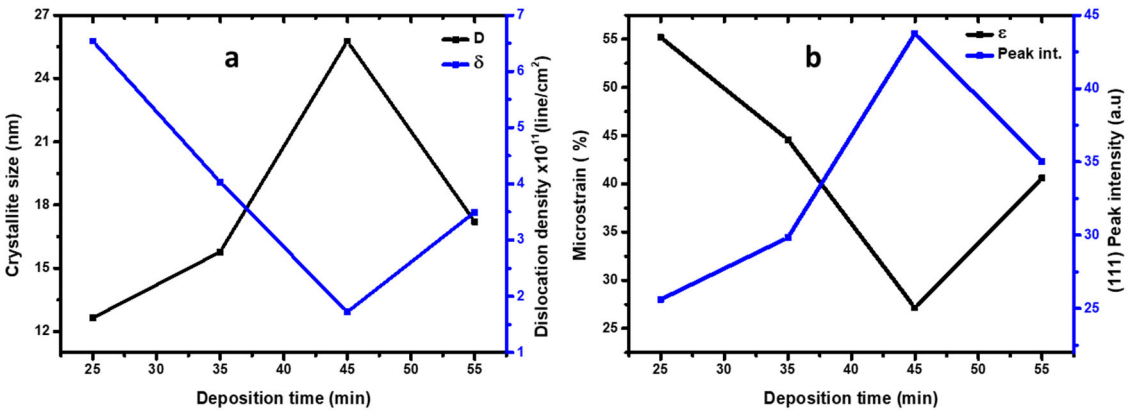


Figure 3. (**a**) Crystallite size and dislocation density versus deposition time, and (**b**) micro-strain and peak intensity versus deposition time.

Figure 3b shows that the CdTe:Se thin film micro strain values changed as the deposition time altered. At 25 min of the deposition period, the microstrain value was 55.0×10^{-2}. Increasing the deposition period to 45 min caused the strain value to decrease to 27.0×10^{-2}, the lowest strain ever measured. A little increase occurred when the deposition time reached 55 min, and the strain was measured at 41.0×10^{-2}. Consistent with previous results published by Danielson et al. [28], our research shows that the lowest

strain, the highest peak intensity of preferred orientation, and the maximum crystallite size D were all measured at 45 min. These findings suggest that 45 min is the ideal CdTe:Se deposition period.

Since strain and dislocation density are the two ways that the dislocation network might manifest in films, a decreasing dislocation density at minutes signifies the production of high-quality films [29]. Sahana et al. [30], Subhash [31], and Funda et al. [32] have published similar studies in which they attribute the improved crystallinity and grain size of the films to a reduction in the micro strain and dislocation density. This results in reduced structural disorder and improved compositional uniformity within the deposited thin film.

3.2. Surface Morphology

The surface profile provides a valuable insight into the quality and grain structure of CdTe:Se thin films. Figure 4 presents SEM images of three representative CdTe:Se films deposited at different durations. The film deposited for 45 min exhibits a surface densely packed with nanoscale grains, indicating superior morphological quality compared to the other samples. As the deposition time increases from 25 to 45 min, notable changes are observed in surface roughness, particle size, and grain morphology. The increased surface roughness and grain growth at 45 min are consistent with the corresponding XRD findings, further confirming the influence of deposition time on the film structure. This implies that the quality of the thin film formed and the deposition time are significantly correlated. For deposition times of 35, 45, and 55 min, the estimated grain sizes of the CdTe:Se thin film samples are 184, 280, and 260 nm, respectively. Since bigger grains can improve light-trapping and absorption capabilities, resulting in higher efficiency in converting sunlight into energy, an ideal grain size that can boost light absorption in the thin film is produced by a deposition time of 45 min. Echendu et al. have published similar work [33].

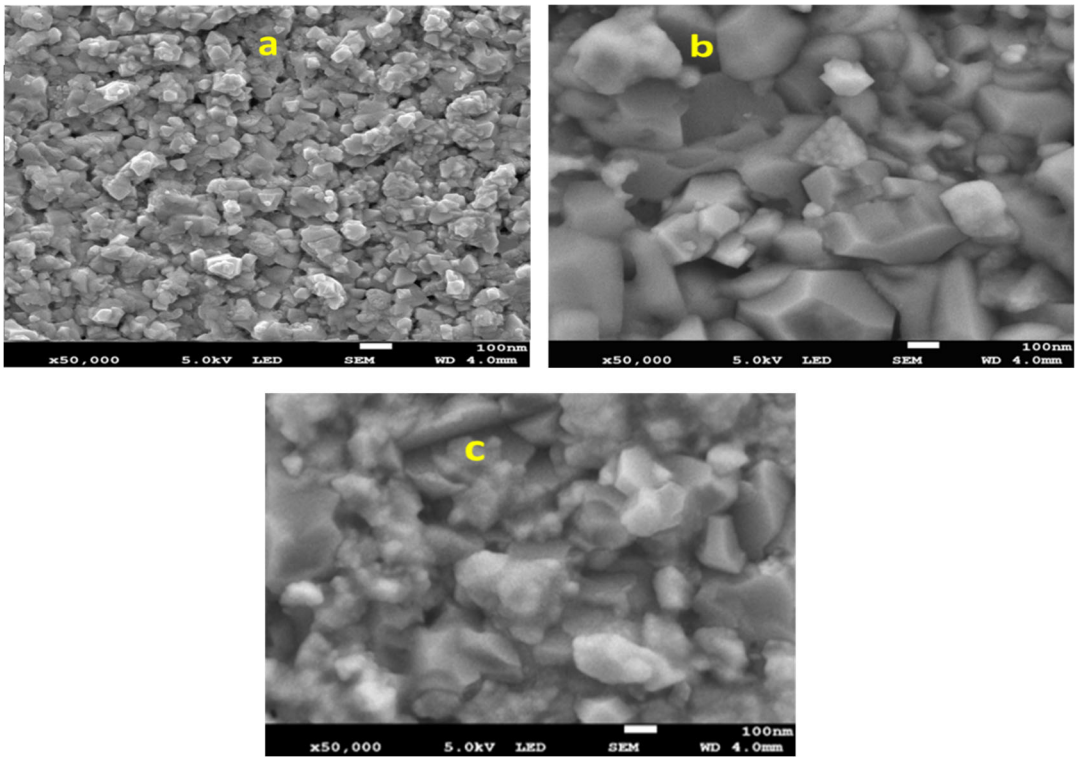


Figure 4. The SEM image of ED—CdTe:Se at deposition time of (**a**) 35 min (**b**) 45 min, and (**c**) 55 min.

Relative film density was estimated through binarized SEM image analysis. The pore area fraction was found to be approximately 7%, corresponding to a relative film density of approximately 93%. Such a high relative density together with a dense grain structure as seen is typical of high-quality films—a prerequisite for efficient charge carrier transport and recombination loss suppression in photovoltaic devices.

3.3. Surface Roughness

Scanning probe microscopy (SPM) was used to analyze the surface roughness properties of CdTe:Se thin films for samples that were produced with varying deposition times. Applications for optoelectronic devices have greatly advanced because of research on surface roughness and topology [34]. The study's objective was to determine how the deposition time affected the films' roughness. In qualitative surface topography investigations, the most often used metrics are mean square surface roughness (Rq) and average roughness (Ra). The average surface roughness for CdTe [35] and CdSe [25] was reported to be 44.2–94.9 nm and 45.5–77.0 nm, respectively, in the literature. When the CdTe:Se thin film was created utilizing the ED approach at a deposition time of 35 min, as shown in Figure 5, the Ra and Rq values were 43.24 and 53.88 nm, respectively. As the growth time was increased to 45 min, Ra and Rq increased to 55.78 and 69.73 nm, respectively. Upon increasing the time to 55 min, Ra and Rq dropped to 47.39 and 59.49 nm, respectively. In order to maximize the possibility of photon absorption, a high surface roughness is required for effective solar cell use. The 45 min deposition time produced the best CdTe:Se absorber material for enhanced performance by producing a film with the largest surface roughness.

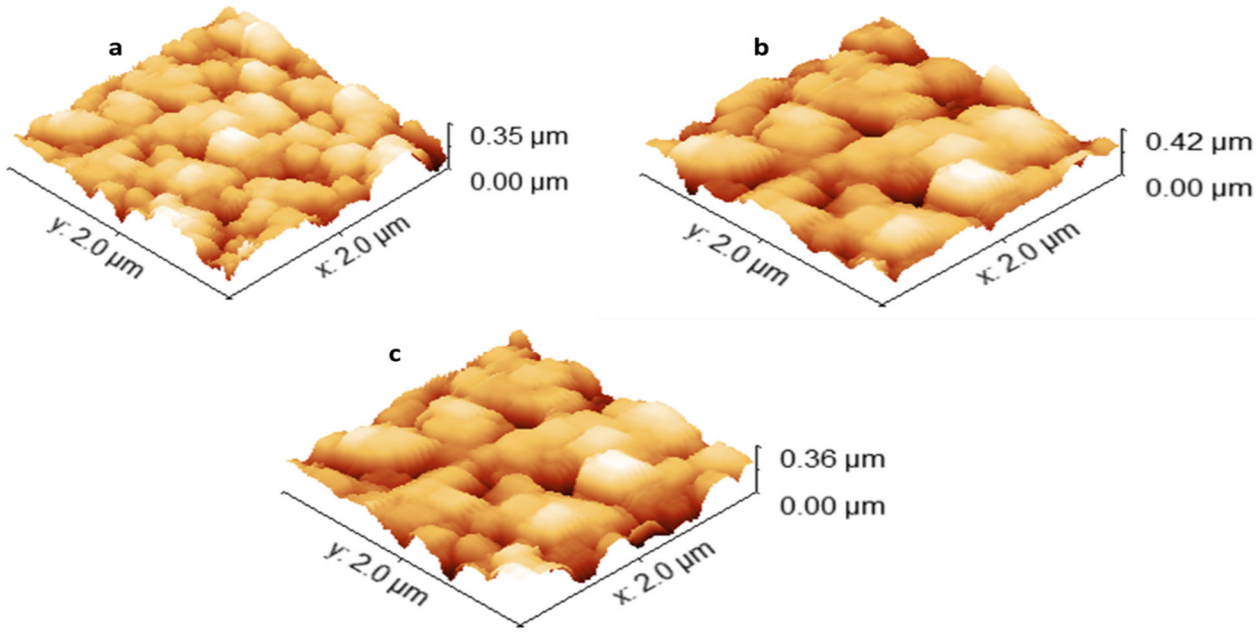


Figure 5. The SPM spectra of CdTe:Se thin films deposited at (**a**) 35 min (**b**) 45 min, and (**c**) 55 min.

3.4. Elemental Composition

The composition of the electrodeposited CdTe:Se thin films was examined using EDS. The EDS spectrum of the CdTe:Se thin film deposited for 45 min is shown in Figure 6. The detection indicates that the grown film on the substrate incorporated all the required elements: Se, Te, and Cd. The sample at the peaks of Sn and O is the ITO glass substrate. The result of the study shows that the elemental composition of Cd, Se, and Te varied with varying deposition times. According to the analysis of the elemental composition provided in Table 2, the percentage of Cd was 51.34%, Te was 44.51%, and Se was 4.15% when there

was a longer deposition time at 55 min. The elemental content of Cd was 50.25% and (Te + Se) elemental content was 49.75%, i.e., close to stoichiometric, when the deposition time was raised to 45 min. The film development was performed at 55 min with the atomic percentage of Cd as 53.11% and the atomic percentage of (Te + Se) as 46.89%. The samples show a stoichiometric elements composition at the time of film deposition of 45 min; so 45 min was selected as the ideal deposition time.

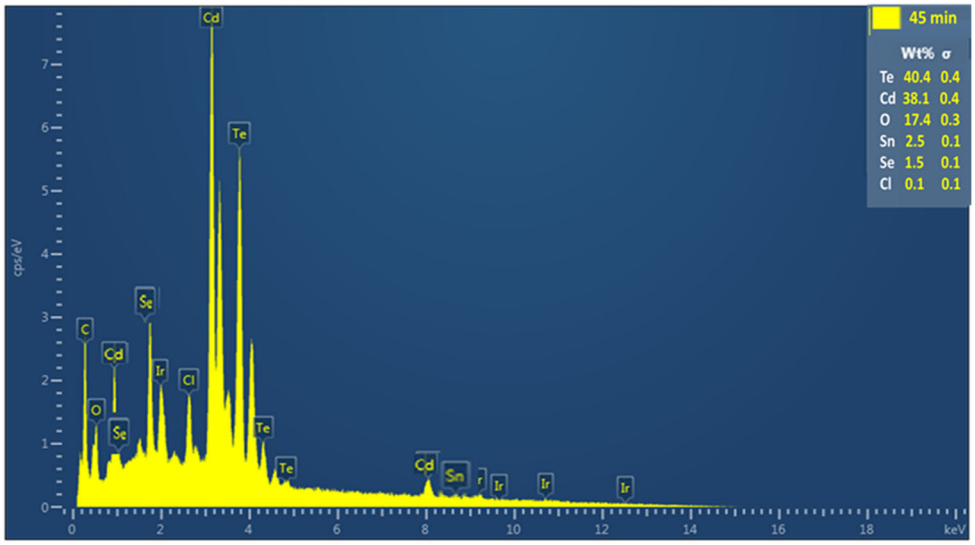


Figure 6. EDS Spectra for the sample deposited at 45 min.

Table 2. Atomic composition of CdTe:Se thin films as a function of deposition time.

Time (min)	Thickness (nm)	Wt.%			At. %					$CdSe_xTe_{1-x}$
		Cd	Se	Te	Cd	Se	Te	Cd/Se + Te	Se/Se + Te	
35	284	50.31	1.36	48.23	53.11	2.04	44.85	1.13	0.04	$CdSe_{0.04}Te_{0.96}$
45	380	47.63	1.88	50.5	50.25	2.82	46.94	1.01	0.06	$CdSe_{0.06}Te_{0.94}$
55	265	49.00	2.78	48.22	51.34	4.15	44.51	1.06	0.09	$CdSe_{0.09}Te_{0.91}$

An estimate of the charge deposited on a conductive substrate may be obtained from the electrodeposition current–time curve. It is therefore possible to use Faraday's law Equation (6) [26] to compute the theoretical thickness (T) of these deposited layers. As can be seen in Table 2, the theoretical thickness increases from 284 to 380 nm with the deposition time.

$$T = \frac{JMt}{Fn\rho} \quad (6)$$

In this context, M represents the molar mass of CdTe:Se ($g \cdot mol^{-1}$), J denotes the average current density applied during the deposition process, t is the total deposition time, F stands for the Faraday constant (96,485 $C \cdot mol^{-1}$), ρ is the density of the CdTe:Se material, T indicates the resulting film thickness, and n refers to the number of electrons transferred per molecule of CdTe:Se during the deposition reaction.

3.5. Optical Properties

Numerous parameters, including doping, size, shape, deposition time and others, have a significant impact on the optical characteristics of solar materials. The deposition time has a significant impact on semiconductor materials' optical characteristics [36]. This work employed a room-temperature UV-Vis spectrophotometer to examine the optical

characteristics of the CdTe:Se thin-film in the wavelength range of 200–1000 nm. The findings show that the gradient of optical absorption gradually rises as the deposition time increases, as shown in Figure 7b. The increase in layer thickness is the cause of this rise in optical absorption. Increase in the deposition time results in an increase in film thickness. At 25 and 45 min of deposition time, respectively, the lowest and maximum optical absorptions were observed. By extending the straight-line section of the graph to the horizontal ($Abs^2 = 0$), the optical bandgap (Eg) was calculated using the graph of the square of absorbance (Abs^2) vs. the photon energy (Figure 7b). In this study, the exact film thickness was not experimentally determined; therefore, we employed the Abs^2 versus hv approach, assuming proportionality to (hv − Eg). This approximation showed good agreement with the standard Tauc method in our previous work and is commonly accepted when α cannot be accurately calculated. As the deposition time rises from 25 to 55 min, the theoretical thickness of the ED-CdTe:Se thin film grows from 284 to 380 nm, whereas Figure 7b illustrates that the energy bandgap reduces from 1.92 to 1.62 eV. This suggests that layer thickness, which results from a longer deposition period, has a substantial impact on the energy bandgap and, in fact, optical characteristics. The results are in line with previously published works by Himanshu et al. [36].

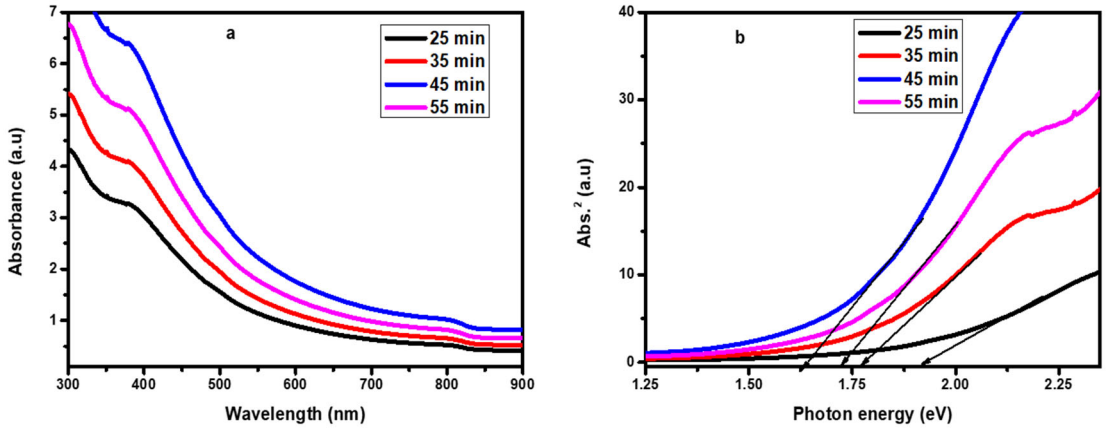


Figure 7. (**a**) Absorbance versus wavelength graph, (**b**) absorbance square versus photon energy (eV).

4. Conclusions

CdTe:Se thin film electrodeposition was investigated at various deposition times and film properties. To electrochemically deposit these thin coatings, a two-electrode approach was employed to streamline the process and save costs. The XRD data were used to determine that the deposited CdTe:Se thin films were polycrystalline with cubic phases. With the crystallite sizes varying in response to the deposition time, the average crystallite size was discovered to have increased from 12.65 to 25.77 nm. The CdTe:Se thin films successfully covered the glass substrate, according to an analysis of the surface morphology, and the deposition time had an impact on the shape and size of the grains. The investigation of the surface roughness showed that the average surface roughness of the film was significantly influenced by the deposition time. The analysis of the optical characteristics showed that the absorbance and energy band gaps altered together with the deposition time, which went from 25 to 45 min. This resulted in a decline in bandgap energy from 1.92 to 1.62 eV. The CdTe:Se thin film demonstrated remarkable light absorption at 45 min, which might greatly enhance the solar cell's overall performance. Overall, the study confirms that the deposition time was a significant determinant in electrodeposited CdTe:Se thin films for solar cell applications. It has been demonstrated that the 45 min deposition time is the most advantageous for the CdTe:Se absorber layer in solar cell applications due to its narrower bandgap than other deposition times.

Author Contributions: Conceptualization, I.M.B., F.B.D., L.F.K., J.J.T. and H.F.E.; methodology, I.M.B. and F.B.D.; formal analysis, I.M.B. and F.B.D.; investigation, I.M.B.; resources, I.M.B., F.B.D., L.F.K., J.J.T. and H.F.E.; data curation, I.M.B.; writing—original draft preparation, I.M.B.; writing—review and editing, L.F.K., J.J.T. and H.F.E.; supervision, F.B.D. All authors have read and agreed to the published version of the manuscript.

Funding: This research was supported and funded by Walter Sisulu University.

Data Availability Statement: The original contributions presented in the study are included in the article, further inquiries can be directed to the corresponding author.

Acknowledgments: The authors are grateful to Walter Sisulu University for its support.

Conflicts of Interest: The authors declare no conflicts of interest.

References

1. Wang, T.; Zhu, X.; Li, W.; Zhang, J.; Wang, W. Incorporation of Metal Selenide Thin Films as the Secondary Absorber in the CdTe Solar Cells. *J. Alloys Compd.* **2020**, *828*, 154415. [CrossRef]
2. Green, M.A.; Dunlop, E.D.; Siefer, G.; Yoshita, M.; Kopidakis, N.; Bothe, K.; Hao, X. Solar Cell Efficiency Tables (Version 61). *Prog. Photovolt. Res. Appl.* **2023**, *31*, 3–16. [CrossRef]
3. Çiriş, A.; Başol, B.M.; Atasoy, Y.; Karaca, A.; Tomakin, M.; Küçükömeroğlu, T.; Bacaksız, E. Effect of Ultra-Thin CdSexTe1−x Interface Layer on Parameters of CdTe Solar Cells. *Sol. Energy* **2022**, *234*, 128–136. [CrossRef]
4. Dharmadasa, I.M.; Alam, A.E. How to Achieve Efficiencies beyond 22.1% for CdTe-Based Thin-Film Solar Cells. *Energies* **2022**, *15*, 9510. [CrossRef]
5. Lingg, M.; Buecheler, S.; Tiwari, A.N. Review of CdTe1-XSex Thin Films in Solar Cell Applications. *Coatings* **2019**, *9*, 520. [CrossRef]
6. Ojo, A.A.; Dharmadasa, I.M. Electrodeposition of Fluorine-Doped Cadmium Telluride for Application in Photovoltaic Device Fabrication. In Proceedings of the Materials Research Innovations; Maney Publishing: London, UK, 2015; Volume 19, pp. 470–476.
7. Suchikova, Y.; Kovachov, S.; Bohdanov, I.; Popova, E.; Moskina, A.; Popov, A. Characterization of CdxTeyOz/CdS/ZnO Heterostructures Synthesized by the SILAR Method. *Coatings* **2023**, *13*, 639. [CrossRef]
8. Silveira Camargo, P.S.; Petroli, P.A.; Andrade de Souza, R.; Kerpen, F.S.; Veit, H.M. CdTe Photovoltaic Technology: An Overview of Waste Generation, Recycling, and Raw Material Demand. *Curr. Opin Green Sustain. Chem.* **2024**, *47*, 100904. [CrossRef]
9. Scarpulla, M.A.; McCandless, B.; Phillips, A.B.; Yan, Y.; Heben, M.J.; Wolden, C.; Xiong, G.; Metzger, W.K.; Mao, D.; Krasikov, D.; et al. CdTe-Based Thin Film Photovoltaics: Recent Advances, Current Challenges and Future Prospects. *Sol. Energy Mater. Sol. Cells* **2023**, *255*, 112289. [CrossRef]
10. Fiducia, T.A.M.; Mendis, B.G.; Li, K.; Grovenor, C.R.M.; Munshi, A.H.; Barth, K.; Sampath, W.S.; Wright, L.D.; Abbas, A.; Bowers, J.W.; et al. Understanding the Role of Selenium in Defect Passivation for Highly Efficient Selenium-Alloyed Cadmium Telluride Solar Cells. *Nat. Energy* **2019**, *4*, 504–511. [CrossRef]
11. Zheng, X.; Kuciauskas, D.; Moseley, J.; Colegrove, E.; Albin, D.S.; Moutinho, H.; Duenow, J.N.; Ablekim, T.; Harvey, S.P.; Ferguson, A.; et al. Recombination and Bandgap Engineering in CdSeTe/CdTe Solar Cells. *APL Mater.* **2019**, *7*, 071112. [CrossRef]
12. Munshi, A.H.; Kephart, J.M.; Abbas, A.; Danielson, A.; Gelinas, G.; Beaudry, J.N.; Barth, K.L.; Walls, J.M.; Sampath, W.S. Effect of $CdCl_2$ Passivation Treatment on Microstructure and Performance of CdSeTe/CdTe Thin-Film Photovoltaic Devices. *Sol. Energy Mater. Sol. Cells* **2018**, *186*, 259–265. [CrossRef]
13. Amir, F.Z.; Clark, K.; Maldonado, E.; Kirk, W.P.; Jiang, J.C.; Ager, J.W.; Yu, K.M.; Walukiewicz, W. Epitaxial Growth of $CdSe_xTe_{1-x}$ Thin Films on Si (100) by Molecular Beam Epitaxy Using Lattice Mismatch Graded Structures. *J. Cryst. Growth* **2008**, *310*, 1081–1087. [CrossRef]
14. Islam, R.; Banerjee, H.D.; Rao, D.R. Structural and Optical Properties of $CdSe_xTe_{1-x}$ Thin Films Grown by Electron Beam Evaporation. *Thin Solid Film.* **1995**, *266*, 215–218. [CrossRef]
15. Muthukumarasamy, N.; Jayakumar, S.; Kannan, M.D.; Balasundaraprabhu, R.; Ramanathaswamy, P. Structural and Optical Properties of Hot Wall Deposited $CdSe_{0.15}Te_{0.85}$ Thin Films. *J. Cryst. Growth* **2004**, *263*, 308–315. [CrossRef]
16. Ablekim, T.; Duenow, J.N.; Zheng, X.; Moutinho, H.; Moseley, J.; Perkins, C.L.; Johnston, S.W.; O'Keefe, P.; Colegrove, E.; Albin, D.S.; et al. Thin-Film Solar Cells with 19% Efficiency by Thermal Evaporation of CdSe and CdTe. *ACS Energy Lett.* **2020**, *5*, 892–896. [CrossRef]
17. Spalatu, N.; Hiie, J.; Valdna, V.; Caraman, M.; Maticiuc, N.; Mikli, V.; Potlog, T.; Krunks, M.; Lughi, V. Properties of the CdCl2 Air-Annealed CSS CdTe Thin Films. In Proceedings of the Energy Procedia; Elsevier: Amsterdam, The Netherlands, 2014; Volume 44, pp. 85–95.

18. Kartopu, G.; Fan, Q.; Oklobia, O.; Irvine, S.J.C. Combinatorial Study of the Structural, Optical, and Electrical Properties of Low Temperature Deposited $Cd_{1-X}Zn_xTe$ ($0 \leq x \leq 1$) Thin Films by MOCVD. *Appl. Surf. Sci.* **2021**, *540*, 148452. [CrossRef]
19. Ling, J.; Zhang, X.; Mao, T.; Li, L.; Wang, S.; Cao, M.; Zhang, J.; Shi, H.; Huang, J.; Shen, Y.; et al. Electrodeposition of CdTe Thin Films for Solar Energy Water Splitting. *Materials* **2020**, *13*, 1536. [CrossRef]
20. Dharmadasa, I.M.; Alam, A.E.; Ojo, A.A.; Echendu, O.K. Scientific Complications and Controversies Noted in the Field of CdS/CdTe Thin Film Solar Cells and the Way Forward for Further Development. *J. Mater. Sci. Mater. Electron.* **2019**, *30*, 20330–20344. [CrossRef]
21. Mahato, S.; Shakti, N.; Kar, A.K. Annealing Temperature Dependent Structural and Optical Properties of Electrodeposited CdSe Thin Films. *Mater. Sci. Semicond. Process.* **2015**, *39*, 742–747. [CrossRef]
22. Alam, A.; Salim, H.; Ojo, A.; Dharmadasa, I.M. Electrodeposited CdTe Solar Cells Using Affordable Low-Purity Cadmium Precursor and Comparison of the Effect of Chemical Purity. *Acad. Mater. Sci.* **2024**, *1*. [CrossRef]
23. Beker, I.M.; Dejene, F.B.; Koao, L.F.; Terblans, J.J. Impact of Deposition Voltage on the Physicochemical Properties of Electrodeposited Se-Doped CdTe Thin Films for Solar Cell Applications. *Ionics* **2025**, *31*, 1–12. [CrossRef]
24. Sali, D.P.; Chaure, N.B. Electrodeposition and Characterization of CdTe Thin Films for Photovoltaic Applications. In Proceedings of the Materials Today: Proceedings; Elsevier Ltd.: Amsterdam, The Netherlands, 2019; Volume 42, pp. 1647–1650.
25. Yimamu, A.U.; Dejene, B.F.; Echendu, O.K.; Werta, S.Z.; Terblans, J.J.; Swart, H.C.; Motloung, S.J. Cathodic Deposition Voltage-Dependent Properties of Electrodeposited Stoichiometric CdSe Thin Films for Solar Energy Application. *Inorg. Chem. Commun.* **2024**, *162*, 112171. [CrossRef]
26. Çiriş, A.; Atasoy, Y.; Tomakin, M.; Karaca, A.; Küçükömeroğlu, T.; Bacaksız, E. Impact of CdSeTe and CdSe Film Deposition Parameter on the Properties of CdSeTe/CdTe Absorber Structure for Solar Cell Applications. *Semicond. Sci. Technol.* **2024**, *39*, 025012. [CrossRef]
27. Zellagui, R.; Dehdouh, H.; Adnane, M.; Akhtar, M.S.; Saeed, M.A. $Cd_xZn_{1-X}S$ Thin Films Deposited by Chemical Bath Deposition (CBD) Method. *Optik* **2020**, *207*, 164377. [CrossRef]
28. Danielson, A.; Reich, C.; Drayton, J.; Bothwell, A.; Shimpi, T.; Sites, J.; Sampath, W. A Comprehensive Material Study of CdSeTe Films Deposited with Differing Selenium Compositions. *Thin Solid Films* **2023**, *768*, 139684. [CrossRef]
29. Balasubramanian, V.; Naresh Kumar, P.; Sengottaiyan, D. Effect of Deposition Temperature on Structural, Optical and Electrical Properties of Copper Bismuth Sulphide (CuBiS2) Thin Films Deposited by Chemical Bath Deposition. *Mater. Sci.-Pol.* **2017**, *35*, 329–334. [CrossRef]
30. Moger, S.N.; Shanubhogue, D.U.; Keshav, R.; Mahesha, M.G. Spectroscopic and Electrical Analysis of Vacuum Co-Evaporated $Cd_xZn_{1-X}Te$ Thin Films. *Superlattices Microstruct.* **2020**, *142*, 106521. [CrossRef]
31. Chander, S.; Dhaka, M.S. Optimization of Structural, Optical and Electrical Properties of CdZnTe Thin Films with the Application of Thermal Treatment. *Mater. Lett.* **2016**, *182*, 98–101. [CrossRef]
32. Akgul, F.A.; Akgul, G.; Yildirim, N.; Unalan, H.E.; Turan, R. Influence of Thermal Annealing on Microstructural, Morphological, Optical Properties and Surface Electronic Structure of Copper Oxide Thin Films. *Mater. Chem. Phys.* **2014**, *147*, 987–995. [CrossRef]
33. Echendu, O.K.; Mbamara, U.S.; Okeoma, K.B.; Iroegbu, C.; Madu, C.A.; Ndukwe, I.C.; Dharmadasa, I.M. Effects of Deposition Time and Post-Deposition Annealing on the Physical and Chemical Properties of Electrodeposited CdS Thin Films for Solar Cell Application. *J. Mater. Sci. Mater. Electron.* **2016**, *27*, 10180–10191. [CrossRef]
34. Mycielski, A.; Wardak, A.; Kochanowska, D.; Witkowska-Baran, M.; Szot, M.; Jakieła, R.; Domagała, J.Z.; Kowalczyk, L.; Kochański, M.; Janusz, G.; et al. CdTe-Based Crystals with Mg, Se, or Mn as Materials for X and Gamma Ray Detectors: Selected Physical Properties. *Prog. Cryst. Growth Charact. Mater.* **2021**, *67*, 100543. [CrossRef]
35. Aliyu, M.M. Towards the Fabrication of Flexible Thin Film CdTe Solar Cells: The Significance of Substrate Surfaces. *Sci. World J.* **2024**, *19*, 245–247. [CrossRef]
36. Himanshu; Dhaka, M.S. Modulating the Structural, Optical, Electrical and Topographical Features of CdSe:Bi Films with Annealing: Role as Promising Absorber to Solar Cells. *Micro Nanostructures* **2023**, *178*, 207570. [CrossRef]

Disclaimer/Publisher's Note: The statements, opinions and data contained in all publications are solely those of the individual author(s) and contributor(s) and not of MDPI and/or the editor(s). MDPI and/or the editor(s) disclaim responsibility for any injury to people or property resulting from any ideas, methods, instructions or products referred to in the content.